Inorg. Chem. **2008**, *47*, 10177−10182

C−H Bond Activation of Coordinated Pyridine: Ortho-Pyridyl-Ditechnetiumhydridocarbonyl Metal Cyclus. Crystal Structure and Dynamic Behavior in Solution

Maaz Zuhayra,*,† Ulf Lützen,† Arne Lützen,‡ Laszlo Papp,† Eberhard Henze,† Gernot Friedrichs,§ and Franz Oberdorfer||

Klinik für Nuklearmedizin, Universitätsklinikum Schleswig Holstein, Campus Kiel, Arnold-Heller-Strasse 9, D-24105 Kiel, Germany, Institut für Physikalische Chemie, Christian-Albrechts-Universität Kiel, Olshausenstrasse 40, D-24098 Kiel, Germany, Kekulé-Institut für Organische Chemie and Biochemie, Universität Bonn, Gerhard-Domagk-Strasse 1, 53121 Bonn, Germany, ZAG Zyklotron AG, Hermann-von-Helmholtz-Platz 1, 76344 Eggenstein-Leopoldshafen, Germany

Received August 11, 2008

The reaction of pyridine with ditechnetium decacarbonyl $[Tc_2(CO)_{10}]$ **(1)** leads to a novel *ortho*-pyridyl-ditechnetium hydrido complex, $[Tc_2(\mu\text{-}H)(\mu\text{-}NC_5H_4)(NC_5H_5)_2(CO)_6]$ (**2**) and its precursor $[Tc_2(\mu\text{-}CO)_2(NC_5H_5)_2(CO)_6]$ (**3**). At ambient temperature **1** was found to react slowly with pyridine to afford the substitution product **3** after 120 h. However, heating the reaction mixture to reflux exclusively leads to the pyridine-ortho-metalated complex **2** in only 30 min. Similarly, complex **3** can be converted completely into **2** upon heating in pyridine for 30 min. Both compounds **2** and **3** were characterized by NMR spectroscopy and X-ray analysis. Both compounds **2** and **3** show a complex dynamic behavior in solution that was investigated by one-dimensional and two-dimensional NMR spectroscopy. Both compounds **2** and **3** show isomerization in solution according to the relative position of the non-bridging pyridine ligands. For **2** the existence of three isomers was shown at equilibrium conditions, **2a** (56%) with *trans-diaxial*, **2b** (38%) with *cis-diaxial*, and **2c** (6%) with *axial−equatorial* arrangement of the non-bridging pyridines. For **3** an equilibrium was detected between two isomers, **3a** (67%) with a *cis-diaxial* and **3b** (33%) with a *trans-diaxial* arrangement of the pyridines.

Introduction

Direct functionalization of C−H bonds is one of the most attractive research subjects in organic and organometallic chemistry.[1] A well-known example is the oxidative addition of aromatic nitrogen bases, like pyridine and substituted pyridines, to various polynuclear metal systems leading to ortho-metalated aromatic nitrogen bases.[2] This reaction has been extensively investigated both with trinuclear osmium and ruthenium carbonyl clusters[3] $[M_3(CO)_{12}]$ (M = Os, Ru) as well as with unsaturated rhenium carbonyl cluster like $[Re_3(\mu\text{-}H)_4(CO)_{10}]^-$.[4] Generally, the initial step is a substitution of one carbonyl group by the base. In this way the geometric conditions for the subsequent addition of the

* To whom correspondence should be addressed. E-mail: mzuhayra@nuc-med.uni-kiel.de.

† Klinik für Nuklearmedizin, Universitätsklinikum Schleswig Holstein.

‡ Kekulé-Institut für Organische Chemie and Biochemie, Universität Bonn.

§ Institut für Physikalische Chemie, Christian-Albrechts-Universität Kiel.

|| ZAG Zyklotron AG.

(1) (a) Carbtree, R. *J. Organomet. Chem.* **2004**, *689*, 4083–4091. (b) Kakiuchi, F.; Chatani, N. *Adv. Synth. Catal.* **2003**, *345*, 1077. (c) Ritleng, V.; Sirlin, C.; Pfeffer, M. *Chem. Rev.* **2002**, *102*, 1731. (d) Delgado, E.; Hernández, E.; Martín, A.; Menacho, M. *Organometallics* **2006**, *25*, 2960–2966. (e) Shiue, T.-W.; Yeh, W.-Y.; Lee, G.-H.; Peng, S.-M. *J. Organomet. Chem.* **2007**, *692*, 3619–3624. (f) Tsuchikama, K.; Kuwata, Y.; Tahara, Y.-K.; Yoshinami, Y.; Shibata, T. *Org. Lett.* **2007**, *9*, 3097–3099.

(2) (a) Ying Li, D. C.; Wang, B.; Xu, S.; Song, H. *Organometallics* **2006**, *25*, 307–310. (b) Zang, F.; Kirby, C. W.; Hairsine, D. W.; Jennings, M. C.; Puddephatt, R. J. *J. Am. Chem. Soc.* **2005**, *127*, 14196–14197.

(3) (a) Machado, R. A.; Rivillo, D.; Arce, A. J.; De Sanctis, Y.; Deeming, A. J.; Órnelas, L. D.; Gonzáles, T.; Atencio, R. *J. Organomet. Chem.* **2005**, *690*, 504–512. (b) Machado, R. A.; Goite, M. C.; Arce, A. J.; De Sanctis, Y.; Deeming, A. J.; Órnelas, L. D.; Oliveros, D. A. *J. Organomet. Chem.* **2005**, *690*, 622–628. (c) Yin, C. C.; Deeming, A. J. *J. Chem. Soc., Dalton Trans.* **1975**, 2091. (d) Johnson, B. F.; Lewis, J.; Pippard, D. A. *J. Chem. Soc., Dalton Trans.* **1981**, 407. (e) Eisenstadt, A.; Giandomenico, C. M.; Frederick, M. F.; Laine, R. *Organometallics* **1985**, *4*, 2033.

10.1021/ic8015063 CCC: $40.75
Published on Web 10/10/2008

Scheme 1. (i) Pyridine, r.t., 120 h; (ii, iii) Pyridine, Δ, 30 min

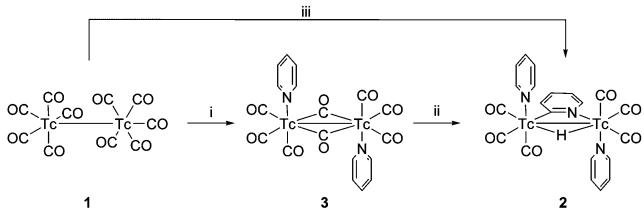

coordinated base are set, and the corresponding activation energy is decreased.[5] In contrast to reactions with saturated metal centers, the addition reactions with unsaturated metal centers occur easily at ambient temperature. However, in both cases the postulated substitution intermediates have not been isolated nor observed yet.[4a] The same is true for the reactive properties of technetium in the case of the low valent carbonyl compounds in CH bond activation which have also not been investigated yet.

In this work we used the long-living isotope ^{99g}Tc ($t_{1/2} = 2.12 \times 10^5$ a),[6] that, unlike the short-living isotope ^{99m}Tc, can be handled in milligram amounts. In this way the synthesized compounds could be isolated in sufficient quantities for X-ray analysis and NMR studies. The oxidative addition reaction of pyridine with ditechnetium decacarbonyl[7] $[Tc_2(CO)_{10}]$ **(1)** leading to the novel *ortho*-pyridyl-ditechnetium hydrido complex $[Tc_2(\mu\text{-H})(\mu\text{-}NC_5H_4)(NC_5H_5)_2(CO)_6]$ (**2**) and its precursor $[Tc_2(\mu\text{-}CO)_2(NC_5H_5)_2(CO)_6]$ (**3**) was investigated. The crystal structures of the new compounds **2** and **3**, as well as their kinetic behavior in solution, are described.

Results and Discussion

1 reacts slowly with pyridine at ambient temperature to give the substitution product $[Tc_2(\mu\text{-}CO)_2(NC_5H_5)_2(CO)_6]$ **3** after 120 h while no further compounds in the reaction mixture could be detected. At elevated temperature the same reaction mixture gives rise to the *ortho*-metalated pyridine complex $[Tc_2(\mu\text{-H})(\mu\text{-}NC_5H_4)(NC_5H_5)_2(CO)_6]$ **2** within only 30 min (Scheme 1). Obviously, the substitution of two carbonyl ligands is quite easy but the substitution of further carbonyl ligands requires harsher conditions that involve a whole cascade of reaction steps including an interesting C−H activation of a coordinated pyridine. This could also be proven by the fact that heating compound **3** in pyridine for 30 min also yields compound **2** quantitatively.

We assume that **3** is formed in situ during reaction iii but is directly converted into **2** by oxidative addition of an *ortho*-CH of the coordinated pyridine molecule followed by the substitution of a carbonyl group by a third pyridine molecule. This hypothesis is in agreement with the conversion of $[Re_2(CO)_8(NC_5H_5)_2]$ and $[Os_3(CO)_{11}(NC_5H_5]$ into their corresponding μ-pyridyl derivatives.[4b,8,9]

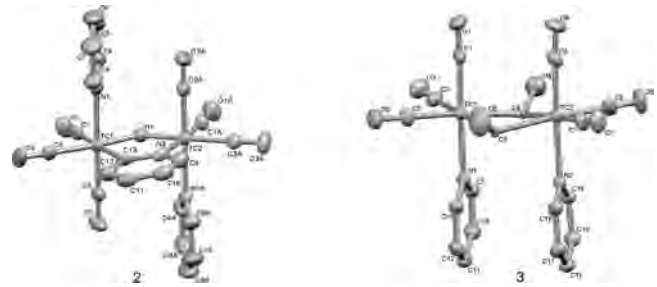

Figure 1. X-ray crystal structures of **2** and **3**.

An interesting aspect in the molecular structures of **2** and **3** is the different arrangement of the two axial pyridines. As expected, compound **2** shows a *trans* arrangement of two *axial* pyridines while **3** has an unexpected *cis-diaxial* arrangement in the crystal structure (Figure 1). Evidently, in spite of the interaction between the π-systems of the μ-carbonyl groups and the pyridine rings the *cis-diaxial* arrangement seems to offer more stability in the crystalline state than the *trans-diaxial* arrangement. Consequently, the μ-carbonyl groups differ from a planar arrangement, with the bond angle, M−C−O = 14° (M is the center of the Tc−Tc-bond).

In compound **2** a third pyridine ring acts as a bridge between the metal centers forming an additional Tc−C bond with the *ortho*-carbon atom. On the opposite site of the Tc−Tc bond a hydrogen atom serves as a second bridge forming a planar five membered Tc−H−Tc−C−N ring. The Tc−Tc and Tc−H distances of 3.23 and 1.82 Å, respectively, are comparable with the corresponding distances in $[Re_2(\mu\text{-H})(\mu\text{-}NC_5H_4)(CO)_8]$.[8] Because of a crystallographic inversion center in the crystal of complex **2**, the N and C atoms of the bridging pyridine, which are connected to Tc atoms, are alternately exchanged, and the measured density of their electrons builds an average between both.

NMR Studies. The isomer distribution of **2** and **3** was investigated with one-dimensional (1D)- and two-dimensional (2D)-NMR spectroscopy as well as Nuclear Overhauser Effect (NOE) measurements after dissolving the crystals in acetone-d_6. The occurrence of different signal sets and the changes of the signal intensities over time indicated the existence of three main isomers **2a**, **2b**, and **2c** of compound **2** and two isomers **3a** and **3b** besides free pyridine in the solution of compound **3**.

Compound 2. The first ^{1}H spectra after dissolving the crystals in acetone-d_6 recorded at 28 °C show aromatic signals and bridging proton signals that indicate the existence of two major isomers **2a** and **2b** and a minimum of two further compounds that are formed, however, in less than 5% in the solution. After equilibration for 24 h only three compounds **2a**, **2b**, and **2c** could be observed (Table 1). A

(4) (a) Beringhelli, T.; Alfonso, G. D.; Ciani, G.; Proserpio, D. M.; Sironi, A. *Organometallics* **1993**, *12*, 4863–4870. (b) Gard, D. R.; Brown, T. L. *Organometallics* **1982**, *1*, 1143. (c) Beringhelle, T.; Carlucci, L.; Alfonso, D. D.; Ciani, G.; Proserpio, D. M. *J. Organomet. Chem.* **1995**, *504*, 15–26.
(5) *Metal Clusters in Catalysis*; Lavigne, G., Kaesz, H. D., Gates, B. G., Guczi, L., Knözinger, H., Eds.; Elsevier: New York, 1986; Chapter 4, S. 43.
(6) See the Safety Note in the Experimental Section.
(7) (a) Hileman, J. C.; Huggins, D. K.; Kaesz, H. D. *J. Chem Soc.* **1961**, *63*, 2953. (b) Hieber, W.; Herget, C. *Angew. Chem.* **1961**, *73*, 579. (c) Knight Castro, H.; Meetsma, A.; Teuben, J. H.; Vaalburg, W.; Panek, K.; Enzing, G. *Organomet. Chem.* **1991**, *410*, 63.
(8) Nubel, P. O.; Wilson, S. R.; Brown, T. L. *Organometallics* **1983**, *2*, 515.
(9) Cotton, F. A.; Poli, R. *Organometallics* **1987**, *6*, 1743.

Table 1. $H^1(C^{13})$ NMR Signal Intensities at Different Times of the Three Main Isomers (**2a**, **2b**, **2c**) of $[Tc_2(\mu\text{-}H)(\mu\text{-}NC_5H_4)(NC_5H_5)_2(CO)_6]$ **2**

	28 °C, [%]					4 °C
isomer/%	0.5 h	1.5 h	3.0 h	7.0 h	23.0 h	240 h (^{13}C)
A	88.0	75.8	64.7	59.3	58.4	56.4
B	8.3	20.7	31.4	36.1	37.3	37.6
C	3.7	3.5	3.9	4.6	4.3	6.0

Table 2. H^1 NMR Bridging Proton Signals (28 °C, Gaussian Deconvolution, after 7 h)[a]

	position (ppm)	width (Hz)	integral (rel.)	integral (H*br*/aromatic)
A	−8.9682	340.20	53.17	0.9/14
B	−9.5656	355.57	41.36	1.1/14
C	−11.4062	716.37	5.48	1.2/14

[a] Aromatic signals/H*br* signals = 14.0/1.03.

bridging hydrogen signal (H*br)* at −9.2 ppm was detected with relative intensity of 1/14 compared to the total integral for the aromatic signals. When Gaussian deconvolution is used, three bridging proton signals could be resolved and the relative integrals of the bridging hydrogen H*br* for **2a**, **2b**, and **2c** fit to the proportion of the aromatic hydrogen signals of **2a**, **2b**, and **2c** (Table 2). In compound **2** the spin systems AA′BB′C for Py1 and Py2 and ABCD for Py3 for all three isomers were detected. All coupling constants are identical for all isomers.

Considerations about Isomers and Geometry. The isomer **2a** with a portion of 88% directly after dissolution should correspond to the measured crystal structure and should have the *trans* arrangement of the *axial* pyridines (Figure 2). For this geometry (racemic mixture) no great differences of the chemical shifts of Py1 and Py2 are expected because their relative environments according to Py3 are very similar and the two pyridines influence each other only slightly. For the also possible *cis-diaxial* isomer **2b** (racemic mixture) it is expected that the pyridine rings, Py1 and Py2, influence each other to a larger extent because their ring currents cause a high field shift of both NMR signals. The bridging Py3 in **2b** has two axial pyridine neighbors (similar to **2a**); therefore, the chemical shifts of its hydrogen signals differ only slightly from the signals of Py3 in **2a.** These expectations fit the NMR data of isomer **2b** which also show that the two pyridines are still able to rotate freely despite of the *cis-diaxial* arrangement. In addition, the NOE peaks (^{1}H NOESY 2D) show all neighboring circumstances (*o*/*m*, *m*/*p*, α/*β*, *β*/*γ* and *γ*/*δ*), and the following important correlations were detected:

aα,**a***2o* **a***β*,**a***2o*(weak) **a***δ*,**a***1o*
bα,**b***2o* **b***δ*,**b***1o*

This means that there are close spatial relationships between H*1o* of Py1 and H*δ* of Py3, as well as between H*2o* of Py2 and Hα of Py3. Therefore, the assignment of both ring systems Py1 and Py2 to the Tc atoms, close to H*δ* and to Hα, could be done. These assignments based on transient NOE effects could also be confirmed by steady-state 1D NOE difference experiments.

Two further *axial-equatorial* combinations (that should show different NMR spectra) for Py1 and Py2 are also possible. In these cases it is to be expected that particularly the α- and *δ*-positions would differ clearly from those of the isomers **2a** and **2b**. These expectations fit the NMR data of isomer **2c**. The NOE signals of **2c** (^{1}H NOESY 2D) suggest also an *equatorial* position of Py2 in solution. In contrast to **2a** and **2b**, the NOE signals of **2c** do not show a spatial neighborhood between H*1o* and Hα, as well as between H*2o* and H*δ*, and the 1D-NOE difference experiments corroborate this, so that Py1 should be in the *trans* position to C-*δ* of Py3 as shown in Figure 2 for isomer **2c**. No exchange effects between **2a**, **2b**, and **2c** were observed up to 40°. Thus the exchange must be very slow compared with the relaxation time T_1 ($t_{1/2} > 10$ s).

A more detailed kinetic analysis of the measured relative concentration-time profiles of isomers **2a**, **2b**, and **2c** was performed to gain insight into the mechanism of equilibration. Starting from a solution containing almost pure *trans-diaxial* isomer **2a**, the mixture reached its final equilibrium composition of 58% **2a**, 37% **2b**, and 5% **2c** with a relaxation time in the order of 100 min. Obviously, the isomers with *diaxial* arrangement of the two pyridine groups are thermodynamically favored. In accordance with the crystal data, the *trans-diaxial* isomer is the dominant species in solution as well.

It can be assumed that the isomers **2a**, **2b**, and **2c** are connected by a cyclic reaction scheme with three reversible reaction steps as outlined in Scheme 3. Rate constants for all reactions were determined from a non-linear least-squares Levenberg−Marquardt fitting algorithm based on the analytical solution of the respective differential equation system.[10] The equilibrium constants of the elementary reaction steps, which were independently determined from the equilibrium concentration values of the different isomers (Table 3), link the corresponding forward and reverse reaction rate constants such that only three rate constants were treated as adjustable parameters to fit the experimental data.

Because of the limited sampling rate, the fast initial increase of the concentration of isomer **2c** could not be resolved, causing the absolute values of the rate constants corresponding to the strongly coupled equilibria between **2a** and **2c**, as well as between **2a** and **2b**, to be less reliable. As can be seen from Figure 2, already the first data point measured after a reaction time of $t = 30$ min yielded a fraction of **2c** close to its final equilibrium value. Nevertheless, as can be concluded from the large rate constant ratios $k_{2a\rightarrow 2c}/k_{2a\rightarrow 2b} > 1$ and $k_{2c\rightarrow 2b}/k_{2a\rightarrow 2b} > 1$ (Table 3), the equilibration of the two main isomers **2a** and **2b** mainly follows the indirect reaction pathway **2a** → **2c** → **2b** rather than the direct pathway according to **2a** → **2b**. In fact, because of the absence of time-resolved concentration data at very short reaction times, it is even uncertain whether there is a direct equilibrium pathway between these two species. In fact, the reaction system according to **2a** → **2c** → **2b** and vice versa, thus completely neglecting the direct pathway, is capable of an adequate representation of the experimental data as well. Increasing the respective rate constants from

(10) Szabó, Z. G. Kinetic Characterization of Complex Reaction Systems. In *Comprehensive Chemical Kinetics*; Bamford, C. H., Tipper, C. F. H., Eds.; Elsevier: New York, 1969; Vol. *2*, The Theory of Kinetics.

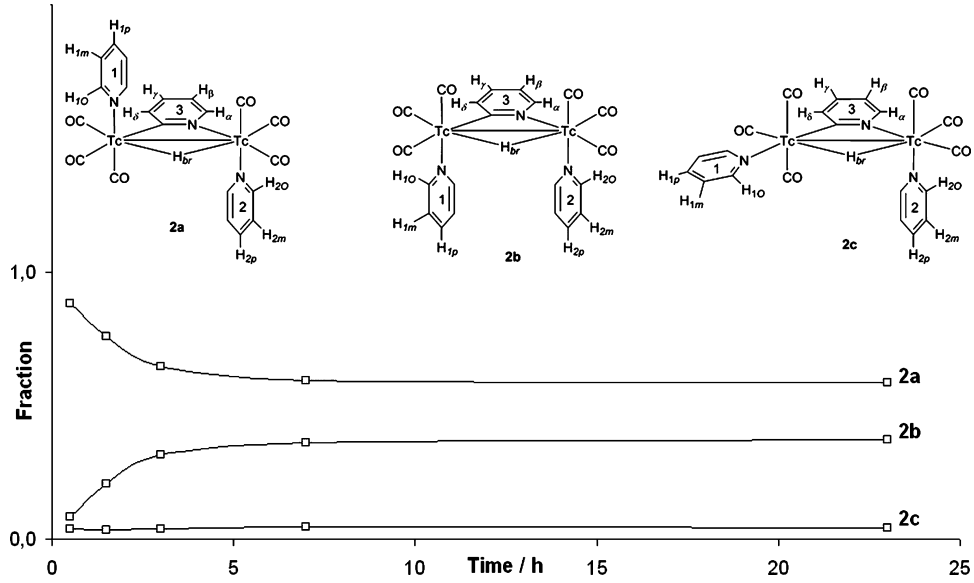

Figure 2. Time profiles for the equilibration of the three main isomers (**2a**, **2b**, **2c**) of $[Tc_2(\mu\text{-H})(\mu\text{-NC}_5H_4)(NC_5H_5)_2(CO)_6]$ **2**.

Scheme 2. Reaction Scheme for the Equilibration of the Three Main Isomers (**2a**, **2b**, **2c**) of $[Tc_2(\mu\text{-H})(\mu\text{-NC}_5H_4)(NC_5H_5)_2(CO)_6]$ **2**[a]

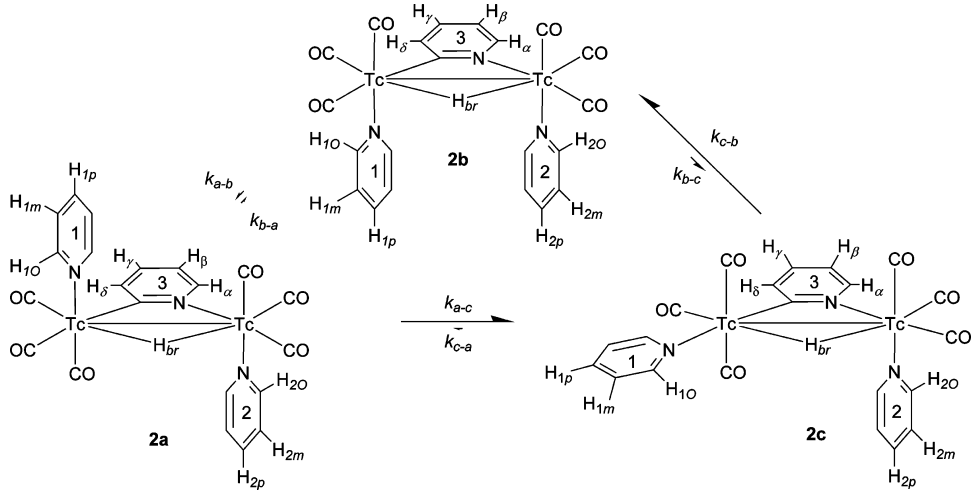

[a] The length of the arrows indicate the respective rate constant values as specified in in Table 3.

Scheme 3. Reversible o-CH Oxidative Addition; First Step of the Isomerization of **2**

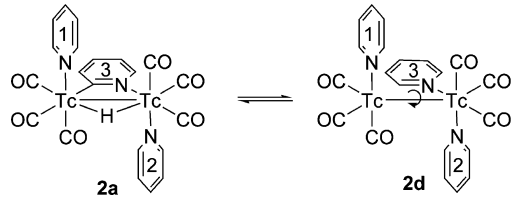

Table 3. Kinetic Analysis of the Equilibration of the Three Main Isomers (**2a**, **2b**, **2c**) of $[Tc_2(\mu\text{-H})(\mu\text{-NC}_5H_4)(NC_5H_5)_2(CO)_6]$ **2**

isomer		fraction of x at time		$K_{xy} = [y]_\infty/[x]_\infty = k_{x\to y}/k_{y\to x}$		
x	y	$t = 0$	$t = \infty$		$k_{x\to y}$ /s^{-1}	$k_{y\to x}$ /s^{-1}
2a	**2b**	100%	58.3%	0.638	3.6×10^{-6}	5.6×10^{-6}
2b	**2c**	0	37.2%	0.121	2.4×10^{-4}	2.0×10^{-3}
2c	**2a**	0	4.5%	13.0	1.3×10^{-3}	1.0×10^{-4}

Table 3 by merely 5% yields concentration-time profiles that are nearly identical to the profiles obtained from a simulation of the full cyclic reaction scheme. In both cases, however,

Table 4. Relative Intensities of the ^{1}H NMR Signals for **3a**, **3b**, and Pyridine after Dissolving Compound **3** in Acetone-d_6 at Various Times

isomer/%	0.25 h	3.0 h	7.0 h	50.0 h
3a	0.58	0.57	0.56	0.52
3b	0.29	0.28	0.27	0.26
pyidine	0.13	0.16	0.17	0.22

the kinetic data clearly indicate that the *cis*−*trans* isomerization (predominantly) passes through the intermediate structure **2c**.

The transformation between the isomers **2a**, **2b**, and **2c** can be explained assuming a reversibility of the oxidative addition of the *o*-CH bond of pyridine. The intermediate **2d** in Scheme 3 is able to rotate freely around the Tc−Tc bond. Starting from isomer **2a** the Tc group bearing Py1 must rotate about 90° or 180°, respectively, to reach the geometrically right position for forming the isomers **2c** and **2b** via subsequent oxidative addition of the *o*-CH of Py3 (Scheme 2).

Compound 3. As shown in Table 4 and Figure 3, the equilibrium between **3a** and **3b** was achieved in less than 15 min after dissolving crystals of **3** in acetone-d_6, and the

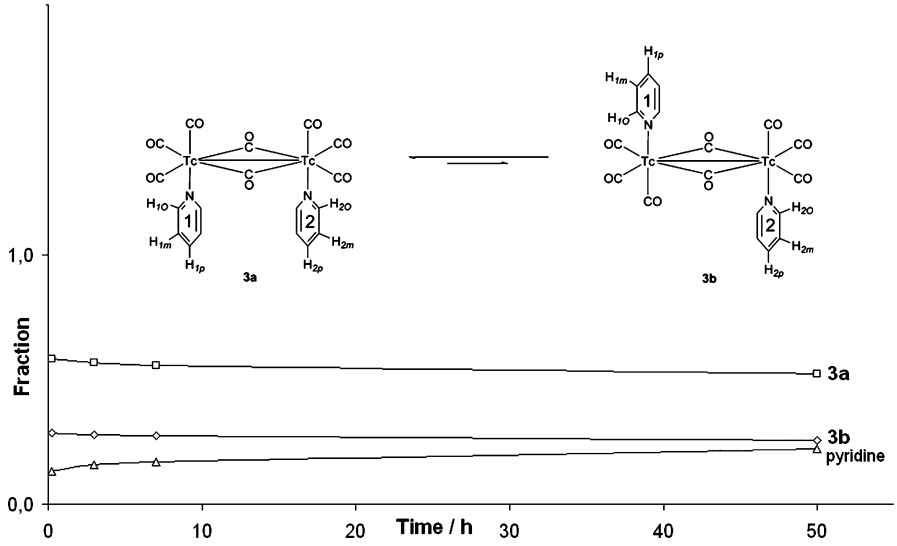

Figure 3. Time profiles and reaction scheme for the equilibration of **3a** and **3b** of $[Tc_2(\mu\text{-}CO)_2(NC_5H_5)_2(CO)_6]$ **3**.

measured relative signal intensities did not change during the measurement interval of about 50 h while the signal intensities of free pyridine were continuously increasing.

For compound **3** the spin system AA′BB′C with identical intramolecular, as well as intermolecular, coupling constants for both isomers was detected. This means that the Py1 and Py2 in both **3a** and **3b** are different only in their chemical shifts because of the different relative spatial orientation. To assign the ^{1}H NMR signals it was important to recognize that the pyridine rings in the *cis-diaxial* conformation influence one another with their ring currents so that a high field shift results for the *cis-diaxial* arrangement compared with the *trans-diaxial* one. Similar to compound **2** the isomerization of **3** could be also explained by rotation around the Tc−Tc bond of a non-CO-bridged intermediate.

Conclusion

In this work we synthesized a first technetium complex in which the activation of pyridine upon coordination of pyridine to the Tc(0) center was observed. The related two novel Tc complexes have been characterized, and their structures have been confirmed by X-ray structure analyses and NMR spectroscopy. In addition, the dynamic behavior in acetone solution (isomerization) was studied, and the composition of the solution at equilibrium was described.

Experimental Section

Safety Note. Caution! *Technetium-99 is a radioactive element. It disintegrates under β-radiation ($t_{1/2}$ = 2,12 × 10^5 a) with a maximum electron energy of 0.29 MeV into the stable Ruthenium ^{99}Ru. The weak β-radiation of Technetium-99 is easily absorbed by the wall of glassware. Therefore handling of small amounts (<50 mg) does not require special shielding. Merely the exclusion of contamination has to be assured, for example, via manipulation in a glovebox.*

Materials. NH_4TcO_4 was purchased from Martin Marietta Energy System, Oak Ridge National Laboratory (U.S.A.), and was used without further purification. Pyridine and sodium metal was purchased from Aldrich. All organic solvents were of reagent grade and were purified by standard methods before use.

Table 5. ^{1}H- and ^{13}C-NMR Chemical Shifts for **2a**, **2b**, and **2c**[a]

	2a	2b	3c
Hμ	−9.97	−9.57	−11.41
Hα	8.630 (156.951)	8.597 (156.834)	8.720 (157.537)
Hβ	7.125 (120.854)	7.119 (120.989)	7.174 (121.533)
Hγ	7.488 (133.372)	7.504 (133.592)	7.413 (133.550)
Hδ	7.899 (141.707)	7.939 (141.819)	(143.251)
H*1o*	8.572 (155.209)	8.211 (154.591)	8.552 (154.318)
H*1m*	7.354 (125.961)	6.923 (125.532)	7.499 (126.708)
H*1p*	7.823 (138.467)	7.532 (138.084)	7.954 (139.663)
H2*o*	8.509 (154.238)	7.959 (153.183)	(150.505)
H2*m*	7.426 ()126.299	6.954 (125.859)	7.344 (124.520)
H2*p*	7.870 (139.011)	7.568 (138.665)	7.753 (136.60)

[a] 500 MHz, Acetone-d_6, TMS, 28°. Spin systems: AA′BB′C (Py1, Py2) and ABCD (Py3) for all isomers: $^3J_{om}$ = 6.46 Hz, $^3J_{mp}$ = 7.66 Hz, $^4J_{o/p}$ = 1.62 Hz, $^3J_{\alpha/\beta}$ = 5.57 Hz, $^3J_{\beta/\gamma}$ = 7.50 Hz, $^3J_{\gamma/\delta}$ = 7.62 Hz, $^4J_{\alpha/\gamma}$ = 1.73 Hz, $^4J_{\beta/\delta}$ = 1.63 Hz, $^5J_{\alpha/\delta}$ = 0.94 Hz.

Synthesis of $[Tc_2(CO)_{10}]$ 1. 1 was prepared according to the method of Knight et al.[5c] NH_4TcO_4 (250 mg, 1.38 mmol), sodium wires (276 mg, 12 mmol), and 15 mL of dry tetrahydrofuran (THF) were put in a small polytetrafluoroethylene (PTFE) lined autoclave. The autoclave was filled with carbon monoxide to a pressure of 5 bar, and afterward the gas was let out. This procedure was repeated three times. After that the autoclave was filled with carbon monoxide to a pressure of 85 bar, and the temperature was increased to 120 °C while the pressure increased to 100 bar. After 72 h the autoclave was allowed to cool down, and the gas was let out. The yellow THF solution was collected, and the residue was extracted three times with *n*-hexane. The solvent was removed under reduced pressure, and the residue was sublimated at 50 °C and 1 mbar to give 250 mg (85%) of white crystals. M.p.: 175−177 °C. IR (cm^{-1}) in *n*-hexane: ν_{CO}, 2067, 2017, 1985.

Synthesis of $[Tc_2(\mu\text{-}H)(\mu\text{-}NC_5H_4)(NC_5H_5)_2(CO)_6]$ 2. 1 (50 mg, 0.105 mmol) was heated under reflux in 2 mL of pyridine for 30 min. The solvent was removed, and the residue was crystallized from a 1:1 mixture of acetone and *n*-hexane. Yield: 56.6 mg (90%).^{1}H NMR (Table 5).

Synthesis of $[Tc_2(\mu\text{-}CO)_2(NC_5H_5)_2(CO)_6]$ 3. 1 (50 mg, 0.105 mmol) was stirred at ambient temperature in 2 mL of pyridine for 120 h. The solvent was removed, and the residue was crystallized from a 1:1 mixture of acetone and *n*-hexane. Yield: 58.7 mg (97%). ^{1}H NMR see Table 6.

X-ray Structure Determination. Single crystals of **2** and **3** were grown from a 1:1 mixture of acetone and *n*-hexane. Diffractometer

Table 6. ^{1}H- and ^{13}C-NMR Chemical Shifts for **3a** and **3b**[a]

	3a	3b
H_o	8.479 (153.10)	8.723 (153.08)
H_m	7.453 (126.41)	7.531 (125.98)
H_p	7.981 (139.96)	7.990 (139.75)

[a] 500 MHz, Acetone-d_6, TMS, 28°; Spin system AA′BB′C: $^{2}J_{o/m} = 6.45$ Hz; $^{3}J_{o/p} = 1.64$ Hz; $^{2}J_{m/p} = 7.63$ Hz.

Siemens (Nicolet Syntex) *R*3*m*/V Diffractometer, Mo Kα (λ = 71.073 pm), graphite monochromator, corrections Lorentz and polarization factor, exp. absorption correction; ψ-scan, $\Delta\psi = 10°$, structure solution direct method, refinement least-squares method, programs SHELXL93, SHELXS-86.

Compound 2. $C_{18}H_{10}N_2O_8Tc_2$, $M_r = 578.280$, crystal dimensions 0.20 × 0.20 × 0.30 mm, orthorhombic, *Pna*2(1), $a = 181.2(2)$, $b = 1035.9(8)$, $c = 121.5(1)$ pm, $\alpha = \beta = \gamma = 90.00(0)°$, $V = 2279.70 \times 10^6$ pm^3, $Z = 4$, $\rho_{(cal.)} = 1.685$ g·cm^{-3}, temperature 200 K, number of reflections for cell refinement 25, scan range $4.5 < 2\theta < 54.0°$, method ω-scan $\Delta\omega = 0.55°$, scan speed $8.0 < \delta\omega/\delta t < 60.0$ °·min^{-1}, number of measured reflections 2614, unique reflections 2614, observed reflections ($I > 2\sigma$) 2265, number of parameters refined 273, maximum of residual electron density 1.16 × 10^{-6} e·pm^{-3}, R1 = 0.052, Rw = 0.146 F^2 refinement.

Compound 3. $C_{21}H_{15}N_3O_6Tc_2$; $M_r = 601.360$, crystal dimensions 0.30 × 0.20 × 0.40 mm, trigonal, *P*3(2)21, $a = b = 1008.8(1)$, $c = 1981.7(6)$ pm, $\alpha = \beta = 90.000(0)°$ $\gamma = 120.000(0)°$. $V = 1746.50 \times 10^6$ pm^3, $Z = 3$, $\rho_{(cal.)} = 1.715$ g·cm^{-3}, temperature 293 K, number of reflections for cell refinement 25, scan range $4.7 < 2\theta < 50.0$ °, method ω-scan $\Delta\omega = 0.60°$, scan speed $7 < \delta\omega/\delta t < 60$ °·min^{-1}, number of measured reflections 2840, unique reflections 2044,observed reflections ($I > 2\sigma$) 1886, number of parameters refined 155 maximum of residual electron density 0.36 × 10^{-6} e·pm^{-3}, R1 = 0.026, Rw = 0.073 F^2 refinement.

1D- and 2D-NMR. Spectra of **2** and **3** were recorded after solution of crystals in acetone-d_6. COSY: sequence COSYLR; T = 28 °C, SW = 1091.7 Hz; TD2 = 1K, TD1 = 256, AQ = 0.469 s, D1 = 2.5 s, P1 = 9.3 μs (90°), P2 = 6 μs, init. D0 = 3 μs, D2 = 10 ms, IN = 916 μs, NS = 8, DS = 2; sine-bell window functions, magn.-mode 2D FT for 512 × 512 matrix, Hz/Pt = 2.13, SR = 8016.8.

NOESY. NOESYYPH using TPPI; TE = 28 °C, SW = 1091.7 Hz; TD2 = 1K, TD1 = 512, AQ = 0.469 s, D1 = 2.6 s, P1 = 9.3 μs(90°), P2 = 6.0 μs, init. D0 = 3 μs, mixing D9 = 1.5 s, V9 = 20% variation, IN = 458 μs, NS = 16, DS = 4; sine-bell shifted π/6, phase-sens.-mode 2D FT for 512 × 512 real matrix, Hz/Pt = 2.13, SR = 8016.8.

ROESY, ROESYC. Compensated ROESY using TPPI and sym-DANTE spin lock, probehead tuning and phase programs adjusted for zero-order phase correction, RD adjusted for first-order phase correction.

(A) ROE21637: TE = 4 °C, SW = 1219.5 Hz; TD2 = 1K, TD1 = 512, AQ = 0.4198 s, D1 = 2.5 s, P1 = 9.8 μs (90°), P2 = 3.0 μs (27.6°), D2 = 13.5 (duty cycle = 3/30 μs = 0.10, B_1 = 2551 Hz); mixing time 390 ms (13000 × 30 μs); RD = 55 μs, init. D0 = 205 μs, IN = 410 μs, NS = 32, DS = 4; sine-bell shifted π/2 phase-sens. 2D FT for 512 × 512 matrix, Hz/Pt = 2.38, SR = 8011.6.

(B) ROA21637: as in A except P2 = 1.5 μs (13.8°), D2 = 10.5 μs (duty cycle = 1.5/22.5 = 0.06667, B_1 = 1700 Hz, RD = 75 μs, init. D0 = 5 μs, mixing time = 540 ms (2400 × 22.5 μs).

CH-Correlation. XHCORRD sequence; TE = 4 °C, SW2 (^{13}C) = 5154.6 Hz; TD2 = 1K, TD2 = 8K, SW1 (^{1}H) = ±513.3 Hz, TD1 = 256, AQ = 0.795 s, P1 = 20 μs (90° ^{1}H), P3 = 7.5 μs (90° ^{13}C), D1 = 3.0 s, D3 = D4 =2.9 ms, init. D0 = 5 μs, IN = 487 μs, NS = 80, DS = 4; zero-fill to SI1 = 512, sine-bell windows, magn.-mode 2D FT, 4K × 512 × 512 matrix, Hz/Pt (^{13}C) = 1.26, Hz/Pt (^{1}H) = 2.01.

Supporting Information Available: X-ray crystallographic files, in CIF format, for the structure determination of **2** and **3** and detailed NMR data. This material is available free of charge via the Internet at http://pubs.acs.org.

IC8015063